AvrPto from the *Pseudomonas* cell. To examine this, *avrPto* deletions CΔ25, CΔ41, and CΔ74 were placed into pBI121 and tested with the *Agrobacterium* transient assay. *Agrobacterium* EHA105 containing *avrPto* induced an HR in 2 days, whereas EHA105 containing the *avrPto* deletion CΔ25 induced an HR after 4 days; the other deletions did not elicit an HR (X. Tang and G. Martin, unpublished results). This suggests that the carboxyl terminal 25 amino acids of AvrPto are not required for secretion from the bacterial cell; this portion of AvrPto may serve as an activation domain, interact with other components in the signaling pathway, or have a role in AvrPto stability.

28. A. Ellingboe, in *Active Defense Mechanisms in Plants*, R. Wood, Ed. (Plenum, New York, 1980), pp. 179–192.
29. I. Brown, J. Mansfield, I. Irlam, J. Conrads-Strauch, U. Bonas, *Mol. Plant-Microbe Interact.* **6**, 376 (1993). S. Young, F. White, C. Hopkins, J. Leach, *ibid.* **7**, 799 (1994).
30. L. Rahme *et al.*, *Science* **268**, 1899 (1995).
31. E. Galyov, S. Hakansson, A. Forsberg, H. Wolf-Watz, *Nature* **361**, 730 (1993); J. Bliska and S. Falkow, *Trends Genet.* **9**, 85 (1993).
32. Levels of protein expression were determined with the use of antibody to LexA (a gift from E. Golemis) for LexA fusion proteins (in pEG202) and antibody to the hemagglutinin (HA) epitope tag (Boehringer-Manheim) for the AvrPto::HA fusion protein (in pJG4-5).
33. We thank L. Dunkle, A. Friedman, S. Gelvin, and K. Perry for helpful comments on the manuscript. Supported, in part, by a Purdue Research Foundation Doctoral Fellowship (D.H.), National Science Foundation grant MCB-93-03359 (G.B.M.) and a David and Lucile Packard Foundation Fellowship (G.B.M.).

Yersinia, *Shigella*, and *Salmonella* (*5*). These pathogens translocate a set of virulence proteins into host cells. Therefore, we considered the possibility that the bacterial AvrPto protein moves across the plant cell wall and plasma membrane where it directly interacts with the tomato Pto protein.

Evidence indicating that AvrPto acts inside the plant cell was obtained by transiently expressing *avrPto* in transgenic *Nicotiana benthamiana* plants transformed with *Pto* (*6*) (Fig. 1). This resulted in necrosis similar to the *Pto*-mediated HR elicited by *P. syringae* expressing *avrPto* and indicated that AvrPto was active within the plant cell. Deletion of 30 amino acids from the COOH-terminus of AvrPto did not eliminate this activity, whereas deletion of 59 amino acids destroyed activity. Activity of the deletion derivatives in the transient expression assays correlated with biological activity in *P. syringae*. These results suggested that the products of the *avr* and *R* genes may interact directly.

We employed the yeast two-hybrid system to directly test this hypothesis (*7*). *Pto*, *Fen*, and *avrPto* coding sequences were expressed as fusions to GAL4 DNA binding (BD) and transcriptional activating (AD) domains. Reciprocal combinations of BD and AD fusions were tested for β-galactosidase reporter gene activity in yeast. Interaction was only observed when the BD::Pto and AD::AvrPto fusions were coexpressed (Fig. 2). Controls did not show any interaction. Furthermore, no interaction was detected between BD::Fen and AD::AvrPto (Figs. 2 and 3A).

To test the biological relevance of the interaction, inactive alleles of *Pto* and *avrPto* were tested. Three inactive *Pto* alleles, *pto6*, *pto7* and *pto11*, were previously identified through mutagenesis of resistant tomato plants (*8*). Sequence analysis revealed single amino acid changes in each mutant allele (Fig. 3B). The mutant *Pto* sequences showed no detectable interaction with AvrPto in yeast. Thus, mutant alleles that confer susceptibility to *Pst* also fail to interact with AvrPto in the two-hybrid system. The two deletions of AvrPto tested in

Molecular Basis of Gene-for-Gene Specificity in Bacterial Speck Disease of Tomato

Steven R. Scofield,* Christian M. Tobias,* John P. Rathjen, Jeff H. Chang, Daniel T. Lavelle, Richard W. Michelmore, Brian J. Staskawicz†

Transient expression of the *Pseudomonas syringae* avirulence gene *avrPto* in plant cells resulted in a *Pto*-dependent necrosis. The AvrPto avirulence protein was observed to interact directly with the Pto resistance protein in the yeast two-hybrid system. Mutations in the *Pto* and *avrPto* genes which reduce in vivo activity had parallel effects on association in the two-hybrid assay. These data suggest that during infection the pathogen delivers AvrPto into the plant host cell and that resistance is specified by direct interaction of Pto with AvrPto.

In plants, resistance to a variety of pathogens is determined by the action of complementary pairs of resistance (*R*) genes in the host and avirulence (*avr*) genes in the pathogen. These gene-for-gene interactions have been observed between plants and a diverse array of pathogens, including viruses, bacteria, fungi, nematodes, and insects (*1*). From genetic analysis it has been proposed that *R* genes recognize an elicitor produced directly or indirectly by the pathogen's *avr* gene, which leads to a resistance response in the infected plant (*2*).

Bacterial speck disease of tomato is caused by *Pseudomonas syringae* pv. *tomato*

(*Pst*). In tomato, resistance to strains of *Pst* that contain the *avr* gene *avrPto* is conferred by the *Pto* gene (*3*). The *Pto* locus encodes a family of related serine-threonine kinases. Among these, *Fen* is active in a parallel pathway that confers sensitivity to the insecticide fenthion (*4*).

R and avr proteins may interact directly, thereby activating plant defenses. For the protein product of *Pto*, this binding would likely occur intracellularly because of its predicted cytoplasmic localization. The activity of many *avr* genes, including *avrPto*, depends on an *hrp* secretion pathway which is similar to the type III secretory systems of

S. R. Scofield, J. P. Rathjen, J. H. Chang, D. T. Lavelle, NSF Center for Engineering Plants for Resistance Against Pathogens (CEPRAP), University of California, Davis, CA 95616.
C. M. Tobias, Department of Plant and Microbial Biology, University of California, Berkeley, CA 94720.
R. W. Michelmore, NSF Center for Engineering Plants for Resistance Against Pathogens and Department of Vegetable Crops, University of California, Davis, CA 95616.
B. J. Staskawicz, NSF Center for Engineering Plants for Resistance Against Pathogens and Department of Plant and Microbial Biology, University of California, Davis, CA 94720.

*These authors made equal contributions to this report.
†To whom correspondence should be addressed. E-mail: stask@garnet.berkeley.edu

Fig. 1. *Agrobacterium tumefaciens* strain A281 (sites 3 to 6) or the nontumorogenic strain C58C1 (sites 1 and 2) containing *avrPto* gene constructs (*10*) were infiltrated into leaves of a *Pto* transformed plant (**A**) or leaves of untransformed *N. benthamiana* (**B**). Expression of *avrPto* (sites 1 and 4), and *avrPto* deletions of 30 (site 6), and 59 (site 3) amino acids off the COOH-terminus was controlled by the CaMV 35S viral promoter in a binary plan transformation vector. An *avrPto* construct (pPtE6) lacking left and right T-DNA borders or a plant promoter (*11*) was also infiltrated (sites 2 and 5). Leaves were photographed 3 days after inoculation.
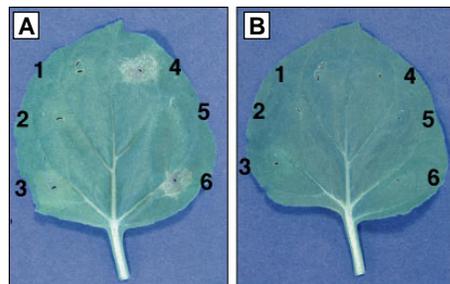
the transient expression assay were examined for their ability to interact with Pto (Fig. 3C). AvrPto Δ30C, which is biologically active, interacted with Pto, whereas Δ59C, which had no biological activity, showed no interaction. Therefore, the binding activity of mutants of both Pto and AvrPto coincides with reduced biological function in vivo.

Because *Fen* is 80% identical to *Pto* at the amino acid level but does not interact with AvrPto, it provides a model for defining the Pto sequences responsible for specific interaction with AvrPto. Reciprocal Fen-Pto hybrid constructs demonstrated that the COOH-terminal 192 amino acids

of Pto contain the residues necessary to confer binding to AvrPto (Fig. 3D). Analysis of a series of *Fen-Pto* gene fusions recombinant at variant residues between amino acids 167 and 239 places the residues responsible for specific binding between amino acids 190 and 213 (Fig. 3E). There are only four variant amino acids in this interval, which also corresponds to conserved kinase subdomain VIII, a region implicated in substrate binding in other kinases (9). Although the series of recombinant molecules was useful for defining a small region of Pto essential for specific interaction, the fact that the hybrid genes displayed reduced β-galactosidase activity

indicates that other residues also participate in binding.

Two invariant residues essential for kinase catalytic activity in Pto were mutated to examine the role of kinase function in the interaction with AvrPto (Fig. 3F). Neither mutant showed detectable interaction with AvrPto. These results suggest that phosphorylation activity of Pto is required for the binding of AvrPto, although it is possible that the engineered mutations may abolish binding by some other effect.

These data suggest that *Pto*-mediated disease resistance involves entry of AvrPto into the plant cell and interaction with the Pto kinase. The high degree of recognitional specificity that is the hallmark of gene-for-gene disease resistance systems is evident at the molecular level. Although the determinants of specificity reside in regions of Pto that correspond to conserved kinase domains involved in substrate recognition, these residues alone are insufficient for mediating interaction with AvrPto. Mutations in residues essential for ATP binding and catalytic activity also eliminate detectable binding to AvrPto. Thus, our analysis shows that alterations in different parts of Pto can eliminate the ability to interact with AvrPto.

Demonstration of direct binding between R and Avr proteins supports a receptor-ligand model for recognition in plant-pathogen interactions. *Pto* is unique among the cloned *R* genes in lacking a leucine-rich repeat (LRR) motif. LRRs are known to mediate protein-protein interactions and are found in some receptor molecules, making them logical candidates for mediating the recognition of avr molecules. *Pto*-mediated resistance does require an LRR protein encoded by the *Prf* gene, located within the *Pto* locus, and it is somewhat surprising that AvrPto interacts directly with Pto. Perhaps Pto and AvrPto form a complex which is then able to interact with Prf. It will be interesting to see if this system represents a unique class of resistance mechanism that utilizes a kinase as the element to determine specificity, or whether there are orthologous kinases participating in other resistance systems.

Isolation of *avr* genes has proven to be a more tractable biological task than cloning plant *R* genes. Our experiments suggest that, at least for systems involving recognition within the plant cytoplasm, it may be possible to use *avr* genes as bait in the yeast two-hybrid system to isolate the corresponding *R* genes from plant cDNA libraries.

Fig. 2. Yeast strain Y190 transformed with various combinations of two-hybrid plasmids were tested for β-galactosidase activity. Plasmids encoding fusions to the GAL4 DNA binding domain are indicated by BD, whereas fusions to GAL4 transcriptional activation domain are denoted by AD. The pair of plasmids encoding BD fusions to murine p53 (BD::p53) and AD fusions to SV40 large T antigen (AD::LTA) serve as controls for the specificity of the Pto-AvrPto interaction (7).
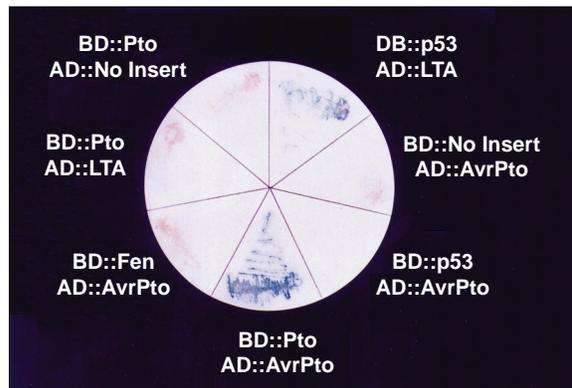

Fig. 3. Analysis of avrPto and Pto interaction. Pto sequences are represented by open boxes, Fen sequences by filled boxes, AvrPto sequences by slashed boxes (12). Numbers and arrows indicate relative positions of amino acids in the sequence (4, 5). Single-letter amino acid codes are used to indicate mutations where relevant. (**A**) Interaction of AvrPto with Pto and Fen. (**B**) Activity of in vivo Pto mutants, pto6, pto7, and pto11 (8). (**C**) Activity of avrPto COOH-terminal deletions. (**D**) Activity of reciprocal Fen-Pto swaps. PF*Bgl*III and FP*Bgl*III. (**E**) Analysis of Fen-Pto fusions. The region shown corresponds to catalytic kinase subdomains VIB-IX (11). (**F**) Effects of amino acid substitution of invariant catalytic residues. Average β-galactosidase activities were determined on at least three colonies from each transformation, with three replicates for each colony (13). Western blot analysis demonstrated that mutant Pto and AvrPto fusion proteins accumulate to similar levels as wild-type fusions (data not shown).
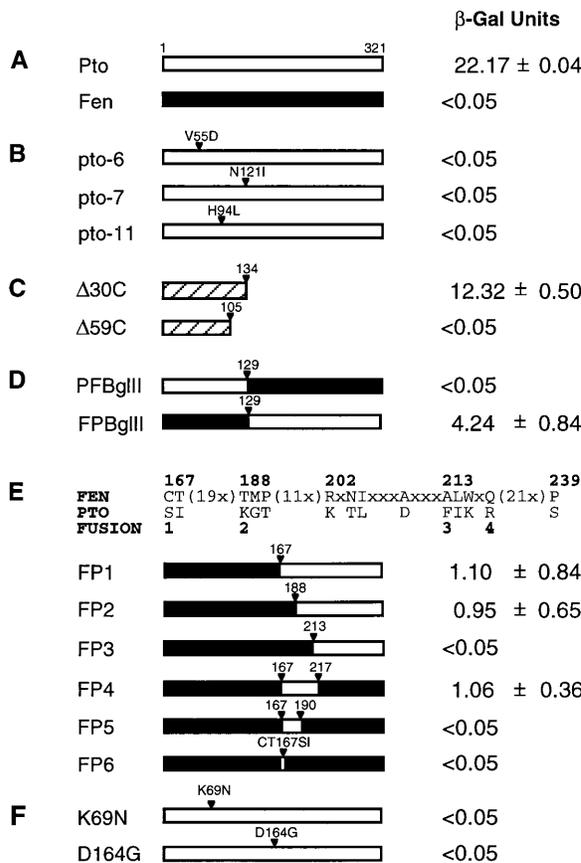
REFERENCES AND NOTES

1. I. R. Crute, *Plant Pathol.* **35**, 15 (1986).
2. A. H. Ellingboe, in *Physiological Plant Pathology*, R. Heitefuss and P. H. Williams, Eds. (Springer-Verlag, New York, 1976), pp. 761–778; N. T. Keen, *Adv.*

Plant Pathol. **1**, 35 (1982); B. J. Staskawicz, F. M. Ausubel, B. J. Baker, J. G. Ellis, J. D. G. Jones, *Science* **268**, 661 (1995).

3. G. B. Martin *et al.*, *Science* **262**, 1432 (1993).

4. C. M. T. Rommens, J. M. Salmeron, D. C. Baulcombe, B. J. Staskawicz, *Plant Cell* **7**, 249 (1995); G. B. Martin *et al., ibid.* **6**, 1543 (1994).

5. J. M. Salmeron and B. J. Staskawicz, *Mol. Gen. Genet.* **239**, 6 (1993); P. B. Lindgren, R. C. Peet, N. J. Panopoulos, *J. Bacteriol.* **168**, 512 (1986); U. Bonas, *Curr. Top. Microbiol. Immunol.* **192**, 79 (1994).

6. C. M. T. Rommens, J. M. Salmeron, G. E. D. Oldroyd, B. J. Staskawicz, *Plant Cell* **7**, 249 (1995).

7. S. Fields and O. Song, *Nature* **340**, 245 (1989); B. Li and S. Fields, *FASEB J.* **7**, 957 (1993); K. Iwabuchi, B. Li, R. Bartels, S. Fields, *Oncogene* **8**, 1693 (1993).

8. J. M. Salmeron, S. J. Barker, F. M. Carland, A. Y. Mehta, B. J. Staskawicz, *Plant Cell* **6**, 511 (1994).

9. S. K. Hanks, A. M. Quinn, T. Hunter, *Science* **241**, 42 (1988); S. Hanks, K. Steven, T. Hunter, *FASEB J.* **9**, 577 (1995).

10. Transient *Agrobacterium*-mediated transformation was performed by pressure infiltration of leaves with *Agrobacterium* at a density of 1 to 2×10^9 cfu/ml. The full-length and delted AvrPto constructs were cloned into the pBIN19 derivative pMD1. Positive clones were introduced into *Agrobacterium* via electroporation.

11. P. C. Ronald, J. M. Salmeron, F. C. Carland, B. J. Staskawicz, *J. Bacteriol.* **174**, 1604 (1992).

12. Mutations were introduced to the *Pto* gene sequence by recombinant polymerase chain reaction with the use of cloned *Pto* and *Fen* templates (D.T.L., J.P.R. and J.H.C., unpublished data). Recombinant PCR products were cloned into the yeast two-hybrid vector pAS2-1 (Clontech) and sequenced before testing. Wild-type and mutant *avrPto* genes were cloned into a pACT2 (Clontech).

13. J. H. Miller, *Experiments in Molecular Genetics* (Cold Spring Harbor Laboratory, Cold Spring Harbor, NY, 1972).

14. We thank D. O. Lavelle, J. Gardner, and J. Luke for DNA sequencing and G. Oldroyd, M. B. Mudgett, S. Barker, V. Szabo, and L. Doyle for comments on the manuscript. Supported by NSF Cooperative Agreement BIR-8920216 to CEPRAP and by CEPRAP corporate associates Calgene, Inc., Ciba Geigy Biotechnology Corporation, Sandoz Seeds, and Zeneca Seeds.

30 August 1996; accepted 22 November 1996

Capturing the Structure of a Catalytic RNA Intermediate: The Hammerhead Ribozyme

William G. Scott*, James B. Murray, John R. P. Arnold, Barry L. Stoddard, Aaron Klug

The crystal structure of an unmodified hammerhead RNA in the absence of divalent metal ions has been solved, and it was shown that this ribozyme can cleave itself in the crystal when divalent metal ions are added. This biologically active RNA fold is the same as that found previously for two modified hammerhead ribozymes. Addition of divalent cations at low pH makes it possible to capture the uncleaved RNA in metal-bound form. A conformational intermediate, having an additional Mg(II) bound to the cleavage-site phosphate, was captured by freeze-trapping the RNA at an active pH prior to cleavage. The most significant conformational changes were limited to the active site of the ribozyme, and the changed conformation requires only small additional movements to reach a proposed transition-state.

After the discovery that RNA can act as an enzyme (*1*), the first three-dimensional structures of an RNA enzyme, the hammerhead ribozyme, were elucidated (*2, 3*). The hammerhead ribozyme is a small self-cleaving RNA derived from a conserved motif found in several satellite virus RNAs that replicate by a rolling circle mechanism. The hammerhead motif consists of three base-paired stems flanking a central core of 15 conserved nucleotides (*4, 5*) (Fig. 1). The conserved central bases are essential for ribozyme activity, as is the presence of a divalent cation.

Both of the previously crystallized hammerhead ribozymes contained modifications to prevent self-cleavage. The first of these contained an all-DNA substrate-analog strand (*2*), and the second, although all RNA, had the active 2′ hydroxyl at the cleavage site replaced with an inert 2′-methoxyl group (*3*). Despite the similarities of the two modified RNA structures, there remained concern that the RNA fold of a catalytically active hammerhead ribozyme might be different, and the question of how an unmodified hammerhead RNA might bind divalent metal ions and catalyze cleavage was still unanswered (*5*).

Time-resolved crystallography allows direct observation of structural changes that occur during an enzyme-catalyzed reaction with an unmodified substrate, provided that a homogeneous chemical population, accumulated throughout the crystal, can be either visualized rapidly or trapped. Intermediate trapping, combined with conventional x-ray data collection, is made possible by arresting the enzymatic reaction chemically or physically (*6*), for example by adjusting a controlling variable such as the pH, by flash-freezing the crystal, or a combination of both.

To obviate the concerns raised about the RNA enzyme-inhibitor structures, we have obtained the x-ray crystallographic structure of an unmodified hammerhead ribozyme-substrate complex, which cleaves in the crystal on introduction of divalent metal ions (Fig. 2). We then used differing pH and freeze-trapping conditions to obtain time-resolved crystal structures of two states of the uncleaved hammerhead RNA. The first state was isolated with a combination of pH inactivation (cleavage is attenuated at pH 5) and flash-freezing, allowing visualization of metal-binding to the ground-state structure in which no cleavage has

W. G. Scott and A. Klug, MRC Laboratory of Molecular Biology, Hills Road, Cambridge CB2 2QH, England.
J. B. Murray and J.R.P. Arnold, Department of Biology, University of Leeds, Leeds LS2 9JT, England.
B. L. Stoddard, Fred Hutchinson Cancer Research Center, 1124 Columbia Street, Seattle, WA 98104, USA.

*To whom correspondence should be addressed.

Fig. 1. The sequence of the hammerhead RNA used and a schematic representation of its structure (*3*). This ribozyme construct employs a 16-nt enzyme strand (red) and a 25-nt substrate strand (yellow). The letters outlined are absolutely or highly conserved in all hammerhead RNAs (*4, 5*). The arrow denotes the self-cleavage site, and the cleavage-site base (C17) is green. The helices are labeled stem I, stem II, and stem III. Watson-Crick and reversed-Hoogsteen bases are denoted with white ovals. Single hydrogen bonds between non–Watson-Crick bases are shown as white dotted lines. Single hydrogen bonds between bases and backbone riboses are shown as pink dotted lines, and the two aromatic stabilization interactions between C17 and the uridine turn of the catalytic pocket are shown as green dotted lines.